CYBER
Pharmacodia AI

CYBER AIDD

WEEKLY REPORT

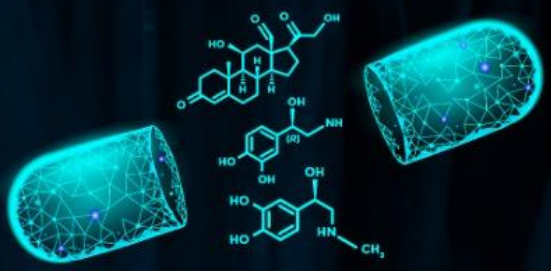

CyberAIDD assisted analysis of drug discovery article Titled "Discovery of 6,7-Dihydropyrazolo[1,5-*a*] pyrazin-4(5*H*)-one Derivatives as $mGluR_2$ Negative Allosteric Modulators with *In Vivo* Activity in a Rodent's Model of Cognition" (Reference: J.Med.Chem.2024,67,17,15569-15585)

CyberAIDD analyzes the discovery and structural optimization of an mGluR2 negative allosteric modulator for regulating mood disorders

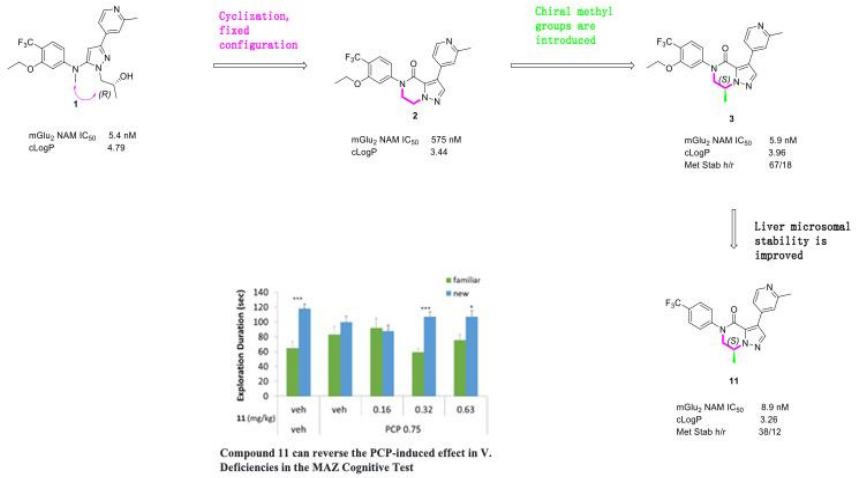

Figure 1. Optimization strategies for lead compounds and the activity of compound 11 in in vivo cognitive models

Allosteric modulators of metabotropic group II receptors (mGluR2 and mGluR3) have been extensively studied for their ability to modulate cognitive and neurological function in mood disorders, although there are currently no approved drugs. In our study, in search of novel and selective mGluR2 negative allosteric modulators (NAMs), we derived a series of 6,7-dihydropyrazolo[1,5-a]pyrazin-4(5H)-one derivatives from the published 1,3,5-trisubstituted pyrazole series. Compounds 11 were selected based on the overall consideration of the ADMET properties and selectivity of the compounds, which resulted in a 100-fold increase in the potency of mGluR2 NAM through structure-activity relationship (SAR) studies. Further constructed pharmacokinetic-pharmacodynamic (PK – PD) relationships showed that **compound 11 occupied the mGluR2 receptor in a dose-dependent manner. In addition, the compound showed in vivo activity in experiments with V-maze as a cognitive model at a dose of 0.32 mg/kg**. Therefore, **compound 11 was selected for further evaluation.**

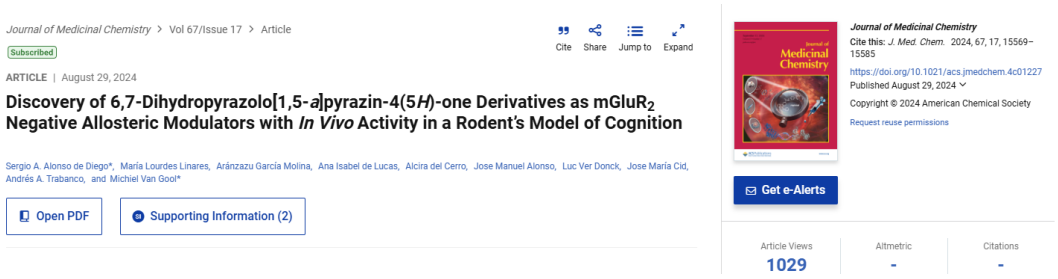

Background:

Glutamate is the most important excitatory neurotransmitter in the brain and acts through ligand-gated

cation channels (ionotropic glutamate receptors) and G protein-coupled glutamate receptors (metabotropic glutamate (mGluR) receptors). The latter are divided into three groups based on sequence homology, pharmacological profile, and signal transduction. The mGluR2 and mGluR3 receptors (group II) are predominantly located in the presynaptic nerve terminals of negatively coupled adenylyl cyclases. Their function is to reduce excitatory glutamate neurotransmission in an activity-dependent manner, thereby creating a negative feedback loop on glutamate release. Experimental studies have shown that mGluR2 and mGluR3 receptors (mGluR2/3 receptors) may play important roles in different brain functions associated with neurodegenerative and neuropsychiatric disorders. Therefore, group II receptor ligands are thought to be potentially useful in the treatment of various central nervous system disorders, including psychosis, mood disorders, and cognitive impairments.

mGluR2/3 receptor antagonists and negative allosteric modulators (NAMs) have been reported to show antidepressant profiles in different models of depression, but their role in cognitive impairment has been poorly studied. A negative allosteric modulator of the mGluR2/3 receptor has been shown to increase long-term potentiation (LTP) in the dentate gyrus of hippocampal slices in vitro, suggesting beneficial effects for learning and memory. Novel object recognition test studies in rats have shown that these compounds have improved long-term recognition memory, working memory, cognitive flexibility, spatial learning, or social recognition memory. In addition, studies focused on Alzheimer's disease (AD) have shown that inhibition of these group II receptors reduced Aβ peptide levels, enhanced hippocampal neurogenesis, and corrected cognitive deficits in AD mice overexpressing the Dutch mutant amyloid precursor protein. These findings have also led to the development of selective mGluR2 and mGluR3 inhibitors, which can accurately define the role of each receptor in different psychiatric disorders and correspond to the potential therapeutic applications of different inhibitors. Therefore, studies on the role and mechanism of action of selective mGluR2 and mGluR3 NAMs in various models of antidepressant and cognitive impairment have recently been published. Several families of NAMs of group II mGlu receptors have been reported. The first mGluR2/3 NAMs described in the literature showed findings similar to those previously described as hybrid mGluR2/3 orthomorphic antagonists in rodent depression and cognitive models, validating the feasibility of an allosteric modulator approach targeting mGlu2/3 receptors. Subsequently, the investigators reported a panel of pyrazolo[1,5-a]pyrimidines as mGluR2/3 NAMs, in which Decoglurant (compound A, Figure 1) entered a phase II clinical trial in patients with major depressive disorder. The compound was well tolerated overall, but development was discontinued due to no significant differences between the active and placebo groups.

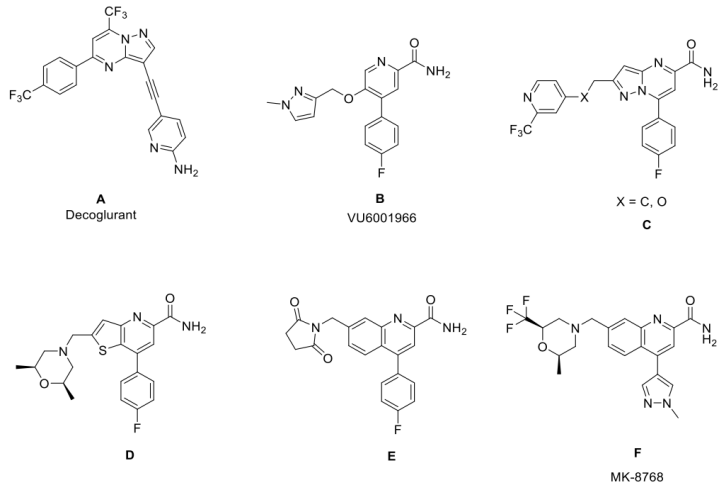

Figure 1. $mGluR_2$ and $mGluR_3$ NAM compounds described in the literature.

Researchers at Vanderbilt University School of Medicine have also made important contributions to the field of glutamate, describing two families of selective NAMs targeting group II mGluR receptors, followed by a series of 4-oxo-1-aryl-1,4-dihydroquinoline-3-carboxamide as selective mGluR2 NAMs. Further optimization of this chemistry identified different series of compounds, including 5-oxomethylene-4-aryl-piperidinamide, pyrazolo[1,5-a]pyrimidin-5-carboxamide, and thieno[3,2-b]pyridin-5-carboxamide with improved central nervous system penetration (**B**, **VU6001966**; **C and D**). A series of 4-arylquinoline-2-carboxamide NAMs with high selectivity for mGluR2 have been reported recently (**E**, **F**). This series of derivatives has shown efficacy in cognitive animal models. In addition, it is interesting to note that DSP-3456 was developed as an mGluR2/3 NAM and is currently in the Phase I phase of anti-depression treatment, although the structural and preclinical pharmacological profile of the molecule has not been disclosed so far.

Results and discussions

We have reported a series of pyrazole derivatives as potent mGluR2/3 negative allosteric modulators (**Compound 1**, Figure 2). This family of compounds showed high lipid solubility (cLogP), which resulted in poor drug properties, resulting in lower free brain exposure in rats.

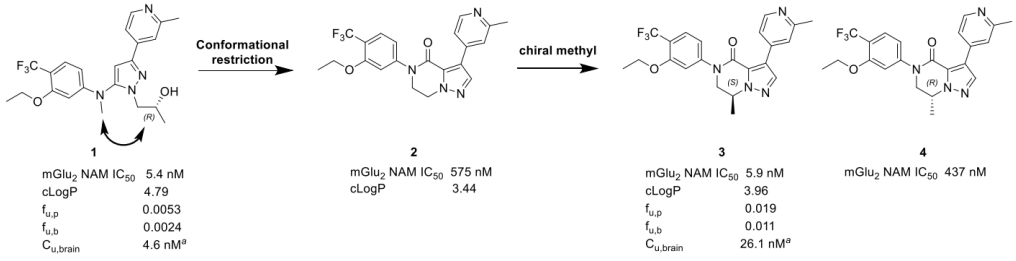

Figure 2. Conformational restriction of $mGluR_{2/3}$ NAM pyrazoles toward the discovery of the 6,7-dihydropyrazolo[1,5-*a*]pyrazin-4(5*H*)-one series. [a] Unbound brain concentration ($C_{u,brain}$) was calculated from a pharmacokinetic study in Wistar rat at 10 mg/kg, 1h after administration (p.o. for compound **1** and s.c. for compound **3**). The bioavailability (F) of **1** was 61%.

To further improve the CNS drug properties of these compounds, we focused on medicinal chemistry optimization by reducing lipid solubility while maintaining single-digit nanomolar potency. Among the different pathways explored, we found that immobilizing the pyrazole series configuration in a 6,7-dihydropyrazol[1,5-a]pyrazine-4(5H)-one core yielded compound 2, which showed a moderate potency (IC50) of 575 nM in the mGluR2 NAM GTPγS assay (Figure **2**). ）。 Although Compound 2 is 100-fold

less potent than Compound 1, it has achieved a significant improvement in fat solubility. In order to retain the methyl group present in the secondary alcohol chain of compound 1, which is not present in the structure of compound 2, compound 3 was synthesized and the potency of the compound was completely restored. The **importance of configuration is confirmed by compound 4, with little improvement in potency observed compared to compound 2. In addition, the lower fat solubility of compound 3 translates to a more than 4-fold increase in free plasma and brain fraction compared to compound 1. Similarly, cell-brain concentrations were increased by more than 5-fold (26.1 nM for compound 3** and **4.6 nM for compound 1**, Figure **2**). Interestingly, this 6,7-dihydropyrazole[1,5-a]pyrazine-4(5H)-one chemical type appears to be a favorable mGlu receptor-binding backbone. In fact, researchers at Vanderbilt University have described in the literature that selective mGluR3 NAMs and mGluR5 PAMs use the same core, but have a different substitution mode than our mGluR2 NAMs. It is very interesting to see that the same core leads to different mGlu receptor affinities through different connectivity modifications, as well as the generation of new pharmacological patterns. However, while the (R)-methyl configuration was preferred in Vanderbilt's analogues for mGluR3 activity, in this work, a more potent compound was obtained using the (S)-methyl configuration. Next, we decided to explore **compound 3 further**, retaining the central core and the right 2-methylpyridine as a template for subsequent explorations. We selected the following compounds (Table 1**)** to discuss trends in the structure-activity relationship between in vitro potency and fat-solubility (cLogP).

Table 1. Functional Activity, *In Silico* Lipophilicity, and Metabolic Stability of the Synthesized $mGluR_2$ NAMs

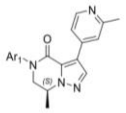

Compd	Ar_1	$mGluR_2$ NAM GTPγS IC_{50} ± SEM (nM)[a]	cLogP[b]	Met Stab h/r[c]
3		5.9 ± 0.2	3.96	67 / 18
5		19 ± 4.5	3.43	61 / 17
6		20 ± 2.5	4.26	n.t.
7		5.1 ± 1.4	3.76	62 / 74
8		12 ± 2.2	3.41	54 / 14
9		1.8 ± 0.4	3.78	63 / 20
10		4.8 ± 0.2	3.69	74 / 38
11		8.9 ± 1.3	3.26	38 / 12
12		26 ± 7.8	3.09	34 / 18
13		240 ± 37	2.52	n.t.
14		513 ± 42	1.81	n.t.
15		480 ± 17	2.88	n.t.
16		794 ± 147	2.83	n.t.
17		998 ± 22	2.38	n.t.

[a]Values are the mean of at least two experiments; a SD < 0.5 was considered as reproducible and therefore accepted. [b]cLogP calculated using Biobyte software. [c]Metabolic stability in human liver microsomes (h) and rat liver microsomes (r) data refer to the percentage of compound metabolized after 15 min at 1 μM in liver microsomes [(1 mg/mL protein)$^{-1}$].

Since in the pyrazole family, double substitution on Ar1 is used to increase activity, we explored the role of ethoxy in compound 3. Substitution of methoxy (**compound 5**) or isopropoxy (**compound 6**) resulted in reduced potency of the compounds, 19 and 20 nM, respectively. On the other hand, substitution of ethoxy

with methyl group (**compound 7**) results in a slight increase in potency, although this is detrimental to metabolic stability in rat liver microsomes that are potential metabolic sites. Substitution with fluorine (**Compound 8**) reduced the potency by a factor of 2 compared to Compound 3, while substitution with a larger volume of chlorine (**Compound 9**) resulted in the most potent compound in this exploration (1.8 nM). Finally, replacing **p-CF3 in compound 9 with chlorine (compound 10**) has a slight adverse effect on potency. In addition, we decided to explore the monosubstituted aryl rings on the bicyclic core (**compounds 11−16**). Thus, complete removal of ethoxy (**compound 11**) maintains potency below 10 nM. This result contrasts with the case of the pyrazole series, which are less restrictive in configuration and the removal of meta-substituents results in a significant decrease in in vitro potency. Further exploration led to a gradual decline in potency by replacing the CF3 group with other electron-withdrawing groups such as Cl, F, and cyano or electron-donor methyl groups. **The activity of the p-CF3 substituent removed in compound 16 decreased significantly, and the** activity decreased by 130-fold compared to compound 3. Finally, **compound 17 has no substituents on Ar1 and its activity decreases to the micromolar range. Interestingly,** the removal of intermediate substituents for compounds 11 and 12 improved metabolic stability in human liver microsomes compared to bisubstituted compounds **3-10.** These subsequent derivatives showed poor human metabolic stability regardless of the electronic properties of the meta-substituents. Next, the structure-activity relationship of the 2-methylpyridyl sequence on the right was explored. For this purpose, three left-sided aryls (compounds 9, 10, and 11) with optimal potency and lipid solubility equilibrium profiles were selected.

Table 2. Functional Activity, *In Silico* Lipophilicity, and Metabolic Stability of the Synthesized mGluR$_2$ NAMs

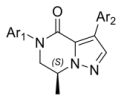

Compd	Ar$_1$	Ar$_2$	mGluR$_2$ NAM GTPγS IC$_{50}$ ± SEM (nM)[a]	cLogP[b]	Met Stab h/r[c]
18			22 ± 8.3	2.76	24 / 11
19			562 ± 157	2.76	n.t. / 20
20			120 ± 22	3.26	n.t.
21			24 ± 0.3	3.76	30 / 4
22			2.9 ± 0.8	4.27	50 / 16
23			6.5 ± 1.7	4.18	61 / 29
24			10 ± 2.5	3.58	33 / 12
25			3.7 ± 0.2	4.10	29 / 5
26			6.6 ± 1.1	4.01	50 / 26
27			5.8 ± 0.7	3.24	33 / 27
28			2.8 ± 0.2	3.75	53 / 29
29			5.1 ± 0.9	3.66	68 / 48

[a]Values are the mean of at least two experiments; a SD < 0.5 was considered as reproducible and therefore accepted. [b]cLogP calculated using Biobyte software. [c]Metabolic stability in human liver microsomes (h) and rat liver microsomes (r) data refer to the percentage of compound metabolized after 15 min at 1 μM in liver microsomes [1 mg(mL protein)$^{-1}$].

The examples in Table 2 were analyzed for structure-activity relationships. First, the removal of the methyl group (compound 18) at the pyridine 2 position is detrimental to the activity. This effect can be seen when comparing compounds 19 and 20, where methyl-substituted compound 20 has improved potency compared to compound 19, demonstrating the importance of this substituent. In addition, switching from a 4-pyridyl substituent to a 3-pyridyl group is detrimental to mGluR2 NAM activity. The insertion of an additional methyl group at position 6 of the pyridine ring resulted in a slight decrease in activity, which **was particularly pronounced by compound 21. While it** is acceptable to replace the 2-methyl group with a 2-methoxy substituent, **compound 24 has comparable activity to compound 11, while compounds 25 and 26 have a slight decrease in NAM activity compared to their matching pairs. Substitution of the 2-methyl group on the pyridine ring** with NH-Me is also permitted. **Compound 27 has a slightly higher potency than 11**, while compounds 28 and 29 have slightly less potency than their counterparts 9 and 10. In terms of metabolic stability, the removal of the pyridine 2-methyl group showed a slight improvement in both species, suggesting that this methyl group may be a metabolic hotspot. However, the introduction of an additional methyl group in pyridine leads to increased metabolic stability, especially in rat liver microsomes. On the other hand, the replacement of the 2-methyl group with the 2-methoxy group or the 2-methylaminogroup in compound 11 did not produce a significant change in metabolic stability. Finally, the loss of metabolic stability of the combination of different substituent pyridine rings with disubstituted aryl rings in human liver microsomes is in the same range as the previously described disubstituted derivatives in Table 1. Among the above-mentioned compounds, we selected those with good mGluR2 NAM activity, reduced lipid solubility, and in vitro stability in human liver microsomes for further study. As shown in Tables 1 and 2, most compounds have good metabolic stability in rats and moderate stability in human liver microsomes. Compounds 11, 24, and 27 were selected after 15 minutes using the criteria of less than 40% compound metabolism, less than 10 nM potency, and less than 4 cLogP in both species. These derivatives were further evaluated, including selectivity, permeability, free fraction, hERG, and CYP inhibition for other mGluR isoforms (Table **3**).

Table 3. $mGluR_2$ and $mGluR_3$ Activity, Unbound Fractions, Intrinsic Permeability and Efflux, hERG and CYP Interactions of Compounds 11, 24 and 27

compd	$mGluR_{2/3}$ Ca^{2+} IC_{50} ± SEM (nM)[a]	SI[b]	f_{up} (h/r)[c]	permeability/Pgp[d]	hERG IC_{50} (μM)[e]	CYPs IC_{50} (μM)[f]
11	12.6 ± 2/229 ± 55	18.2	0.11/0.12	21.0/1.0	>10	7.9 (2C9) others >10
24	12.3 ± 1.5/200 ± 50	16.3	0.05/0.05	14.4/1.3	>10	4.0 (2C9) others >10
27	23 ± 5.2/257 ± 77	11.2	0.14/0.12	19.1/1.3	7.8	all >10

[a]Inhibition measured by glutamate-induced Ca^{2+} mobilization in HEK293 cells stably transfected with human $mGluR_2$ and $mGluR_3$. [b]Selectivity index. [c]Unbound fractions in human (h) and rat (r) plasma were determined by Rapid Equilibrium Dialysis (RED Device, Thermo Fisher Scientific, Geel, Belgium). [d]*In vitro* passive permeability using LLC-PK1-MDR1 cells. Permeability experiments were conducted at a single concentration (1 μM) in a Transwell system with an incubation time of 120 min. The apical-to-basolateral (A → B) transport in the absence (AB−) or presence of the P-gp inhibitor Elacridar GF120918 (AB+) was measured, and permeation rates (apparent permeability) of the test compounds ($P_{app} \times 10^{-6}$ cms^{-1}) were calculated. The ratio AB+/AB− gives an idea of the efflux potential (P-gp value). [e]Experiments were performed using HEK293 cells stably transfected with the hERG potassium channel. Whole-cell currents were recorded with an automated patch-clamp system (PatchXpress 7000A). [f]Tested in a CYP450 panel containing 3A4, 2C8, 2C9, 2D6, 1A2, and 2C19.

Its selectivity relative to other mGluR isoforms was determined using in vitro Ca2+ flow experiments. As shown in Table **3, compounds 11**, **24, and 27 maintained low double-digit** nM mGluR2 receptor activity in human Ca2+ experiments. The mGluR2 selectivity of these three compounds relative to mGluR3 was higher than 10-fold, and compound **11 was the most selective compound in the series. In addition, in all other** mGluR receptor subtypes, no activity was observed when tested down to 10 μM (data not shown). Studies of the free fraction of the compounds in human and rat plasma were carried out, and as shown in Table 3, the measured free fractions in human and rat plasma were in the moderate range, ranging from slightly more than 10% free for compounds 11 and 27 to 5% free for compound 24. Compounds 11, **24, and 27 were tested in an in vitro passive permeability assay and all showed excellent intrinsic permeability**

and low signs of P-glycoprotein-mediated efflux. These compounds were also evaluated in the hERG channel patch-clamp assay and showed no correlated inhibition. In addition, compounds exhibit good characteristics in the CYP450 inhibition panel, where compounds **11 and 24 exhibit weak 2C9 inhibition. Although the characteristics of the three compounds selected in the different experiments described above were very similar, compound 11 was selected as the lead compound for this series based on its excellent mGluR2 NAM activity and the highest mGluR2/mGluR3 selectivity**. To further evaluate whether compound 11 selectively acts on the mGluR2 receptor, it performed 10 μM trials at CEREP for approximately 60 different receptors. The results showed that compound **11 exhibited more than 500-fold selectivity for mGluR2 over other studied targets.**

Intravenous and oral pharmacokinetic studies and histokinetics in rats

Compound 11 is administered to Wistar rats intravenously (IV) in solution form and orally (PO) in suspension form at a dose of 2.5 mg/kg to study its pharmacokinetic profile. In addition, the distribution and exposure levels of compounds in the brain were determined. The calculated pharmacokinetic parameters are shown in Table 4.

Table 4. Mean Pharmacokinetic Parameters in Plasma and Brain of Compound 11 in Rat, after Intravenous and Oral Administration at 2.5 mg/kg[a]

route-matrix	C_{max} (ng/mL)	t_{max} (h)	AUC_{last} (ng·h/mL)	CL (mL/min/kg)	$t_{1/2}$ (h)	Vdss (L/kg)	F (%)
IV-plasma[b]			3660	10.7	6.5	5.67	
PO-plasma[c]	304	4	3033[d]		3.7		100
PO-brain[c]	827	2	7738[d,e]		4.3		

[a]Wistar rats. [b]Administration as solution in 20% HP-β-CD, mean (n = 3). [c]Administration in a water + Tween suspension. [d]24 h. [e]Value in ng·h/g.

The time-plasma concentration curve of compound 11 after intravenous injection showed that its volume of distribution (Vdss) was 5.67 L/kg, indicating that it had a significant distribution outside the plasma with a lower clearance rate (see Table **4**), resulting in a longer half-life (t1/2) for intravenous injection. When administered orally, the compound exhibits very good absorption characteristics with high bioavailability (F), but the absorption rate is slower and lasts longer, resulting in a plateau-like concentration curve for 4 hours post-dose. In addition, the compound was higher in plasma and brain at the highest concentration (C_{max}) and AUC to last detection (AUC_{last}). Similarly, the plasma and brain concentration time curves are parallel as shown in Figure 3, indicating that the plasma and brain are in equilibrium. The brain-to-plasma ratio is 2.6, confirming that compound 11 has very good brain penetration. Free parameters are also calculated in the brain, where compound 11 has $a_{fu,brain}$ value of 0.039 in rats and a $kp_{,uu}$ of 0.85.

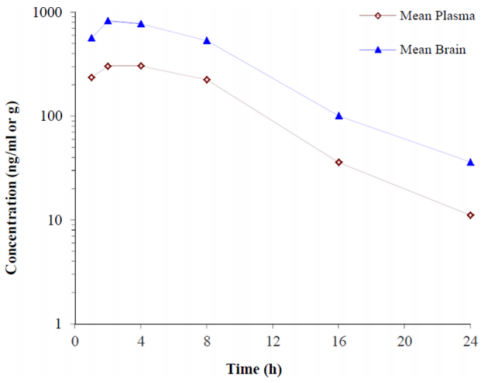

Figure 3. Plasma and brain concentrations of compound **11** after oral administration at 2.5 mg/kg in Wistar rats. Administration in a water + Tween suspension.

Target binding: receptor occupancy

The in vitro mGluR2 receptor occupancy assay is designed to assess whether compound 11 occupies the mGluR2 receptor in vivo. Dose-response experiments are performed to measure the ED50 values occupied by the rat mGluR2 receptor 1 h after 1 h of oral administration of compound 11. In this study, the mGluR2 PAM [3H]JNJ-46281222 previously developed by our team was used to measure the binding of compound 11 to the mGluR2 receptor in vitro. As shown in Figure 4, **compound 11 occupies the mGluR2 receptor in a dose- and time-dependent manner, with an ED50 value of 2.5 mg/kg in rats**.

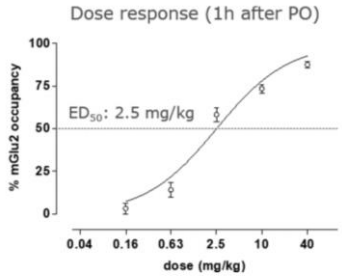

Figure 4. *Ex vivo* $mGluR_2$ receptor occupancy by compound **11** in function of dose using [^{3}H]JNJ-46281222 (1 h after PO dosing).

In vivo assessment: V-maze cognitive test

Finally, the in vivo pharmacological properties of compound 11 were investigated in the V-maze test, which is a validated cognitive model. The V-maze test is a two-trial short-term visuo-spatial working memory task based on spontaneous exploration of the new arm and the familiar arm in a two-arm maze. The performance of this task can be interfered with by low doses of phencyclidine (PCP), making it impossible for the animal to distinguish between the new arm and the familiar arm. When control animals (treated with a vehicle of the test compound and a vehicle of PCP) showed a strong exploratory preference for the new arm in the second trial, the PCP-treated mice no longer statistically significantly distinguished between the two arms. Based on the ED50 value of 2.5 mg/kg shown in the rat receptor occupancy experiment, PCP-challenged rats were pretreated with doses of 1.25, 2.5, and 10 mg/kg of compound 11 in the preliminary experiment. In this preliminary experiment, reversal of PCP-induced defects was observed at all tested doses, therefore, compounds were also administered at 0.16, 0.32, and 0.63 mg/kg to calculate the minimum effective dose. As shown in Figure 5, while PCP persistently disrupted the rats' preference for exploration of the new arm, compound 11 reversed this perturbation dose-dependently at 0.32 mg/kg and above, showing an exploratory preference for the new arm. These data may support the compound's procognitive role in this

rodent model of visuospatial working memory.

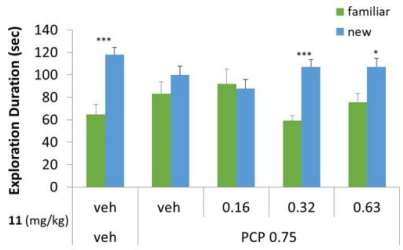

Figure 5. Effect of compound **11** (mg/kg p.o., 4 h prior to test) on exploration times of the new vs the familiar arm by male Long Evans rats in the absence or presence of PCP (0 (= veh) or 0.75 mg/kg s.c., 0.5 h prior to test) in the V-maze.

Notably, despite the ED50 value of 2.5 mg/kg in the receptor occupancy experiment, evidence of activity was observed at a dose of 0.32 mg/kg in the V-maze test. Given these encouraging in vivo results and the overall characteristics described herein, **compound 11 was selected for further evaluation in our mGluR2 NAM project.**

summary

We have discovered a new 6,7-dihydro-5H-pyrazolo[1,5-a]pyrazine-4-one family of compounds that are potent and selective mGluR2-NAMs. **Compound 11 was selected as the lead compound for further development. This compound exhibited excellent physicochemical,** ADME, and pharmacokinetic properties in rats. In addition, in vitro receptor occupancy studies showed that **compound 11 occupied the mGluR2 receptor in a dose-dependent manner after systemic administration, demonstrating target binding and an excellent PK-PD relationship. In addition, compound 11** exhibits activity in vivo in the visuo-spatial working memory task. From a safety perspective, **compound 11 has demonstrated a good safety profile in cardiovascular testing and is selective for a range of receptors. Due to its overall properties, compound 11 was selected for further evaluation and results will be published in due course. In addition to this work, additional research is underway around this family of compounds with a view to enhancing potency and other physicochemical,** ADME, and pharmacokinetic properties, with results to be announced in due course.

source: 10.1021/acs.jmedchem.4c01227

1. Combined with the idea of drug design, CyberSAR excavates the active structure reported in the literature and patents, and uses CyberSAR to facilitate and quickly obtain the target structure of interest of R&D personnel for developing ideas, and the target mGluR2 in this paper is exemrated as follows

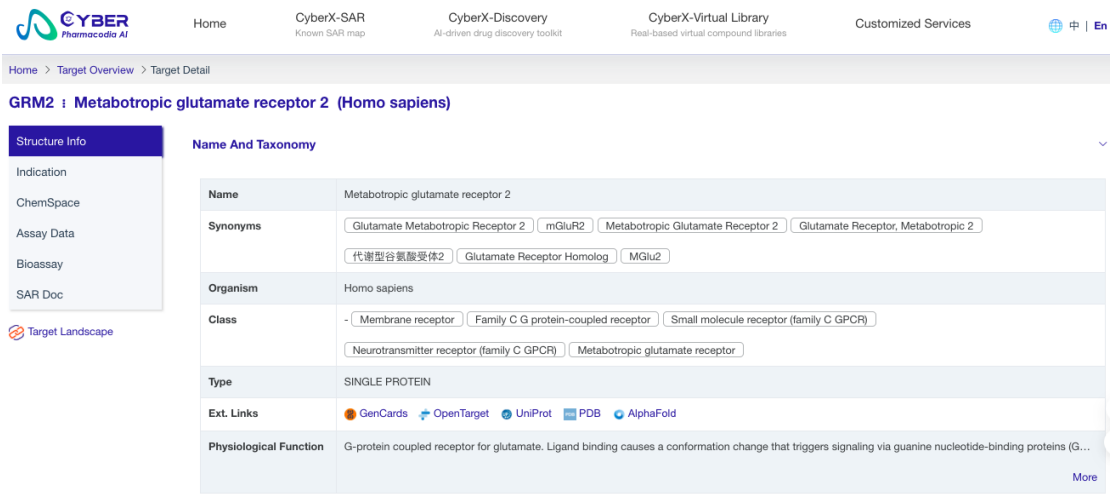

2. Select the cascade "Cluster Structure View" tab under the "Chemical Space" option tab in the target interface, and the molecules with experimental test activity related to the target included in the CyberSAR platform can be displayed in the form of "parent nuclear structure clustering". Among them, "highlighted in green" refers to the active molecular structure of IC50 < 1000 nM in the in vitro enzyme and cell activity test experiments reported in the literature, the specific experiments, the experimental results and the experimental sources.

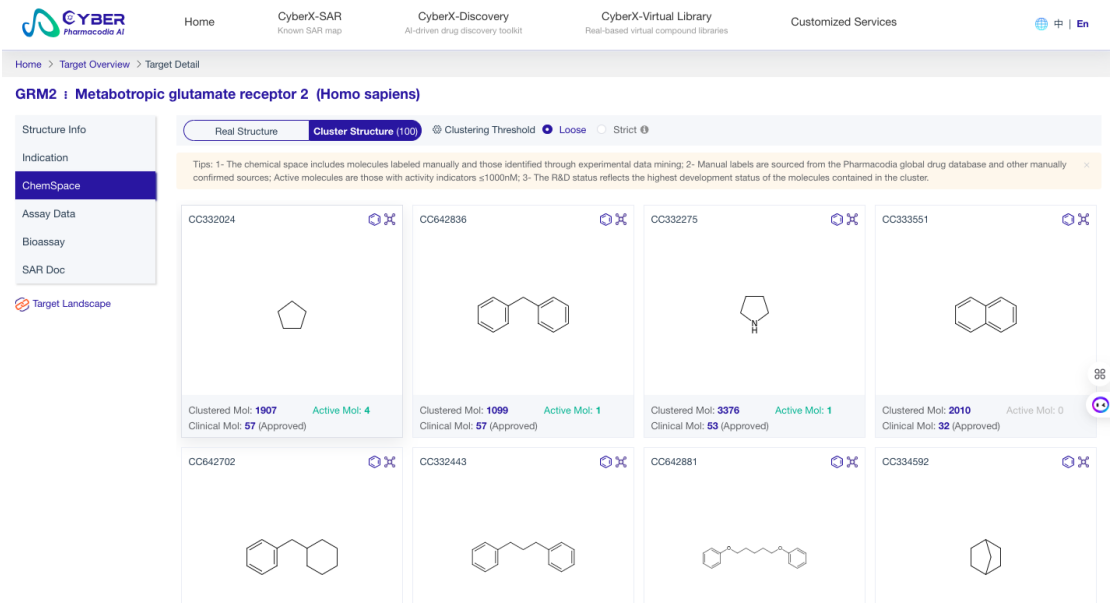

3. Select the cascade "Real Structure View" tab under the "Chemical Space" option tab in the target interface, and the molecules with target-related experimental test activity included in the CyberSAR platform can be displayed in the form of "R&D stage timeline". Among them, the green color highlights the potential Hit.

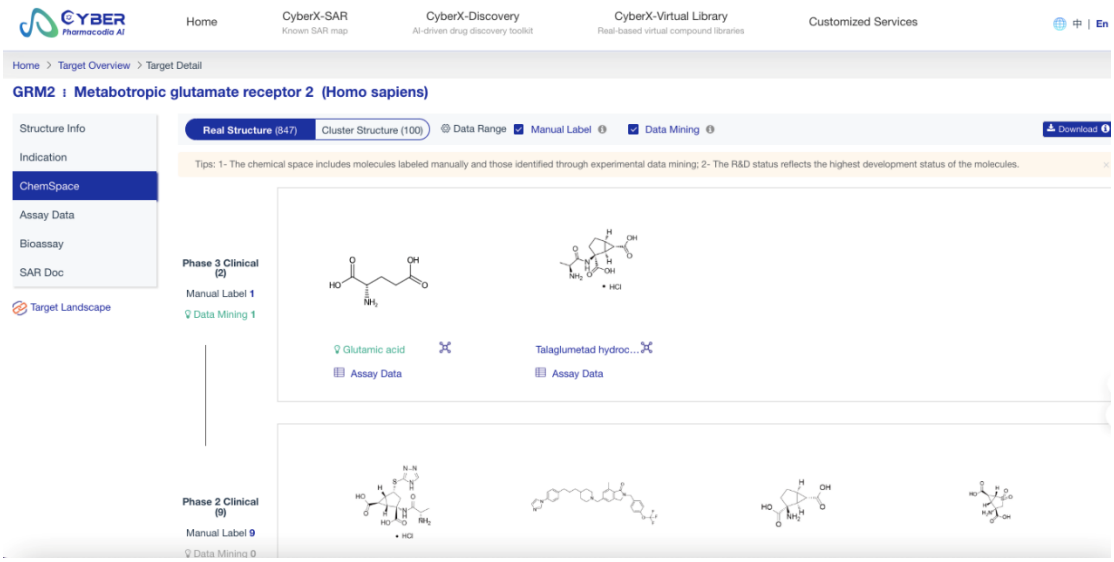

4. Select the "Indications" option label in the target interface, and you can visually and intuitively analyze all kinds of big data collected.

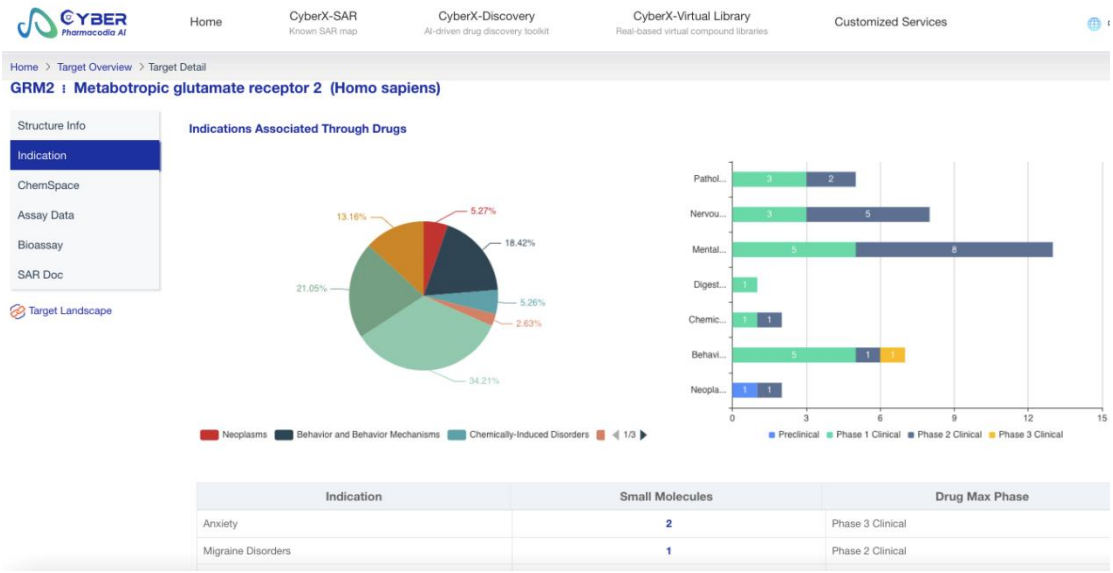

To Explore Cyber-AIDD further Login on your computer using the below Link

https://cyber.pharmacodia.com/#/homePage

For further assistance contact us,

For a free trial, Contact us on

Anil Ranadev
+91 9742627845
anil_ranadev@saspinjara.com

Aravind P
+91 9619076286
aravind.p@saspinjara.com

Sachin Marihal
+91 9538033363
sachin.marihal@saspinjara.com

Chetan S
+91 7022031061
chetans@saspinjara.com